Turkish Journal of Electrical Engineering & Computer Sciences

http://journals.tubitak.gov.tr/elektrik/

Research Article

Turk J Elec Eng & Comp Sci
(2022) 30: 2688 – 2706

doi:10.55730/1300-0632.3963

Modeling and validation of the thermoelectric generator with considering the change of the Seebeck effect and internal resistance

Mehmet Ali ÜSTÜNER, Hayati MAMUR*, Sezai TAŞKIN
Electrical and Electronics Engineering, Engineering Faculty, Manisa Celal Bayar University, Manisa, Türkiye

Received: 17.05.2022 • **Accepted/Published Online:** 25.10.2022 • **Final Version:** 28.11.2022

Abstract: Thermoelectric generators (TEGs) produce power in direct proportion to the temperature difference between their surfaces. The Seebeck coefficient and internal resistance of the thermoelements (TEs) that make up the TEGs change depending on the temperature change. In simulation studies, it is seen that these two values are kept constant. However, this situation prevents approaching the data of TEG in real applications. In this study, a TEG Simulink/MATLAB® model has been developed to capture real TEG module data, which considers changing of both the Seebeck coefficient and the internal resistance depending on the temperature difference change. To achieve this aim, a commercially available TEG data used in also academic studies has been used. A boost converter with a perturb and observe (P&O) maximum power point tracker (MPPT) algorithm has been designed to maximize the TEG power. The TEG Simulink/MATLAB® model data are compared with commercially available TEG data at different temperatures. The error between the actual values and the simulation results, and the mean absolute percent errors (MAPEs) are calculated. The open circuit voltage and short circuit current error rates of the designed TEG module are 0.125% and 0.256%, respectively. The MAPE values of the designed model are 0.5104%, 0.7837%, and 2.0952% for 30 °C, 50 °C, and 80 °C cold surface temperatures, respectively. In addition, simulations are made in order to see the effect of temperature-dependent parameters in a TEG system built using the designed model. While the simulations made with the designed model give realistic results, with the simulations made with constant coefficients, up to 2.63% more power is obtained than the capacity of the system, contrary to reality. Simulation and validated results show that this new TEG Simulink/MATLAB® model gives more realistic results.

Key words: Thermoelectric generator, Seebeck coefficient, internal resistance, Simulink model, maximum power point tracking, boost converter

1. Introduction

Thermoelectric generators (TEGs) are used for waste heat recovery systems. They are semiconductor solid-state devices, and convert the temperature difference between their surfaces into electrical energy, directly [1]. The Seebeck effect is a phenomenon first introduced by Thomas Johann Seebeck in 1821. This phenomenon states that an electric potential arises when the output terminals of two different materials are brought together at different temperatures [2]. In order to increase the voltage generated from TEGs, p- and n-type thermoelements (TEs) are connected electrically in series and thermally in parallel to increase thermal conductivity [3]. TEGs stand out with their longevity, no gas emission, no maintenance cost, no chemical reaction, and low thermal energy potential [4]. They are used as small power sources of electrical energy to recover electrical energy from

*Correspondence: hayati.mamur@cbu.edu.tr

waste heat and increase energy efficiency [5]. The power obtained from TEGs depends on the temperature difference and the properties of the semiconductor material [6]. The temperature difference varies according to the environment of the installed system.

Studies on semiconductor material properties are available in the literature [7]. Since the biggest disadvantage of TEG systems is their low efficiency, TEGs must be operated with a performance close to their full capacity [8]. The full capacity operation of TEGs is related to taking the maximum power from the TEGs through a load [9]. According to the maximum power theorem, when the load value is equal to the internal resistance value of the TEG, the maximum power can be obtained through the load [10]. Besides, when the load is connected directly to the terminals of the TEG, the efficiency of the TEG decreases if the internal resistance of the TEG and the load resistance are not equal. To avoid impedance imbalance [11], the converters that are capable of both maximum power point tracking (MPPT) and power regulation are used together with TEGs [12]. Therefore, boost converters with the MPPT algorithm are used to operate the TEG at the possible maximum power point (MPP). The task of the boost converter connected between the TEG and the load is to perform the impedance matching by working with the duty cycle tuned by the MPPT algorithm [13].

Figure 1 shows the block diagram of a TEG system. In these systems, which are established to obtain energy, power is delivered through the load. However, in order for the delivered power to be maximum, a converter has to be used between the load and the TEG. In this study, a boost converter, which is frequently used in the literature, is preferred to match the internal resistance of the TEG with the load resistance. In order for the boost converter to perform this operation, a PWM signal must be sent to the switching element of the converter. The characteristic of the PWM signal is determined by the duty cycle produced by the MPPT algorithm, which operates using the voltage and current information obtained from the TEG.

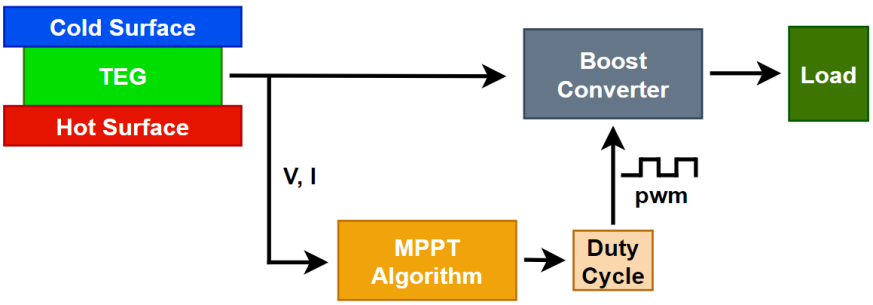

Figure 1. Block diagram of a TEG system.

Different Simulink® models designed for TEGs are available in the literature. Tsai and Lin [14] designed a user-friendly interface with a dialog box similar to the Simulink® library. In this design, which is prepared based on the mathematical model, each parameter should be defined as a function. Similarly, Kennedy [15] used current and voltage functions in the TEG model available on the file exchange within Mathworks. Burnet et al. [16] proposed a detailed and well-organized Simulink® model for TEGs. In their study, the authors stated that the deviations seen in the simulations were caused by the temperature-dependent parameters such as the Seebeck coefficient [17]. Photoon and Wichakool [18] validated a TEG module they modeled with simulations. However, they did not mention the Seebeck coefficient in the model they designed. In addition, they used a fixed value that they calculated as a result of measurements in estimating the internal resistance of TEG. Faria et al. [19] used the datasheet data of the TEG module in their study where they modeled the operation

of TEG to simulate the power generation process. In their study, parameters such as internal resistance and Seebeck coefficient were kept constant since the simulation was carried out at a certain temperature. El-Shahat and Bhuiyan evaluate the performances of different MPPT algorithms in their studies. However, there is no detailed information about the Simulink/MATLAB® model of TEG that they used in their studies because they evaluated the performance of MPPT algorithms [20].

When the Seebeck coefficients and internal resistances of the TEG modules used in TEG systems change depending on the temperature, maximum power can be obtained by performing the impedance matching process through the converters used in the system. This happens automatically in real life due to the nature of materials. However, in order to obtain more realistic results from simulations in the virtual environment, the events that occur automatically in nature must also be modeled.

In this study, a TEG module is modeled in Simulink® using the module's manufacturer data. Since many studies work at a constant temperature, the internal resistance and Seebeck coefficient of the TEG, whose change is not taken into account, are included in the model to change with temperature. In this way, simulation results that are closest to the results of any TEG system that can be installed with the TEG module are obtained. The main purpose of the study is to design a model that can obtain the closest results to the results produced by the TEG module in real life. Many existing TEG models can provide an insight into performance comparisons of MPPT algorithms. However, values kept constant due to parameters that are not modeled under variable operating conditions may deviate the simulation results from the actual results. On the other hand, models that include changes in operating conditions can be complex. This situation may be difficult to understand for researchers who are just starting to work on TEG systems. This study includes the design stages of a simple TEG Simulink/MATLAB® model designed using direct manufacturer data.

The designed model includes the change of internal resistance at different temperatures in the manufacturer's data, as well as the change of the Seebeck coefficient against temperature, which is not in the manufacturer's data and also changes with temperature. In this respect, the biggest advantage of the model is that it uses temperature-dependent parameters along with its simplicity. In addition, other advantages are that it is an easy-to-understand model and can be easily used in different series-parallel connection combinations according to the desired power. On the other hand, this model is designed according to a TEG module named TGM-199-1.4-0.8. In this context, it is a disadvantage that the model is designed according to a special TEG module. However, since the structure, the number of pn pairs, and materials of each module are different from each other, it is quite natural that different information for different modules is included in the model while the model is being designed. Another disadvantage of the model is that the data in the manufacturer's data is processed and integrated into the model. At this stage, it is necessary to model the internal resistance and Seebeck coefficient curves that change with temperature. In addition, in cases where there is no information about the Seebeck coefficient as in the manufacturer's data of the module used in this study, obtaining the Seebeck coefficients by using the information in the manufacturer's data requires a separate computational load. Nevertheless, curve models can be easily obtained with a not very complicated programming knowledge. After all, once the module is modeled, it can be used without any problems and without making any changes.

This model differs from other models in the literature because it includes the parameters of internal resistance and the Seebeck coefficient, whose values change with temperature, and because of its simplicity. Moreover, since the curves of change with temperature of these parameters are modeled with information directly from manufacturer data rather than mathematical functions and used numerically in comparison tables, they are less complex and do not require users to enter extra information into the model.

In the second section of the study, the working principle of TEGs is explained. The technical features of the TEG module referenced for the designed Simulink® model and the technical features of a TEG system designed with this module are mentioned. The third section includes the MPPT principle and the P&O algorithm. Then, in the fourth section, the design parameters of the boost converter designed according to the TEG system specifications are explained. The fifth section includes the modeling process of the Simulink® model. The simulation results and discussion take place in the sixth section and finally the seventh section is the conclusion section.

2. Thermoelectric generators

TEG modules made of TE materials generate a voltage directly proportional to the temperature gradient [21]. One of the features of the TEs that make up the modules is that they can be connected to each other in different ways. TEG module can be designed in a structure suitable for the surface, and output power can be increased with connection types [22]. TEs are linked in series form to increase output voltage, electrically. They also are combined in parallel form to increase thermal conductivity, thermally. When there is a temperature gradient between the surfaces of the TEG module, a voltage occurs between the output terminals of the module. This voltage is obtained as power through a connected load at the output terminals of the TEG module. TEs are made by joining the terminals of two kind of materials with opposite Seebeck coefficients. The voltage at the open ends of the TE is expressed as follows [23]:

$$V_{out} = N\alpha_{pn}\Delta T, \tag{1}$$

where N is the number of serials connected TEs, α_{pn} is the Seebeck coefficient of TE ($VK^{-}1$) and $\Delta T = T_H - T_C$ is the temperature gradient between the two TEG surfaces in K. Both voltage and internal resistance of TEG modules, which are formed by connecting TEs in series with each other, increase in proportion to the number of TEs. The total voltage generated from the TEG module is expressed in (1). The internal resistance of the TEG module consisting of series TE resistors is as in (2).

$$R_{int} = NR_{TE}. \tag{2}$$

The electrical energy obtained from TEG modules is supplied as power through a load resistor connected to the output of the module. The power delivered from the TEG module is expressed in terms of the output voltage, V_{out}, the internal resistance of the module, R_{int}, and the load resistance, R_L, as follows:

$$P = V_{out}^2 \frac{R_L}{(R_{int} + R_L)^2}. \tag{3}$$

Just as TEG modules are a combination of TEs, TEG systems are built by connecting TEG modules to each other in different combinations. R_{int} of the TEG system changes according to the way the TEG modules are connected to each other. For example, in a TEG system consisting of five TEG modules connected in series, the total internal resistance would be five times the internal resistance of the TEG module. At the same time, the output voltage of the system is five times the voltage produced by the TEG module. Similarly, TEG systems, which consist of TEG modules that can be connected in parallel, generally consist of a dependent voltage source and R_{int} of the TEG, as seen in Figure 2 [24]. Since the voltage generated from the TEG system are linked to the temperature and temperature gradient, TEG is referred to as the dependent source in the electrical equivalent circuit of the TEG.

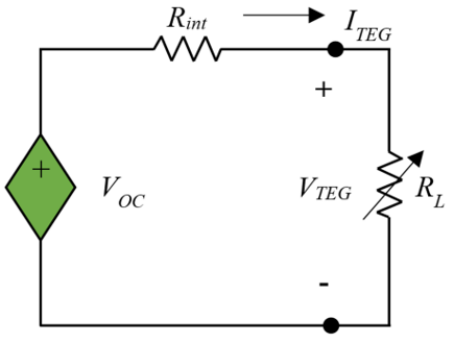

Figure 2. Electrical equivalent circuit.

When the I-V and P-V graphs of a typical TEG shown in Figure 3 are examined, the slope of the power is zero at the maximum power point (MPP) where the power delivered from the TEG is maximum. That is, the derivative of power with respect to the voltage at MPP is zero, and it is formulated as:

$$\left.\frac{dP_{TEG}}{dV_{\text{out}}}\right|_{\max} = \frac{V_{\text{OC}} - 2V_{\text{out}}}{R_{\text{int}}} = 0 \tag{4}$$

When (4) is solved, it is concluded that the output voltage of TEG at MPP is half of the open-circuit voltage. This also means that maximum output power is provided when R_{int} of the TEG and R_L are equal.

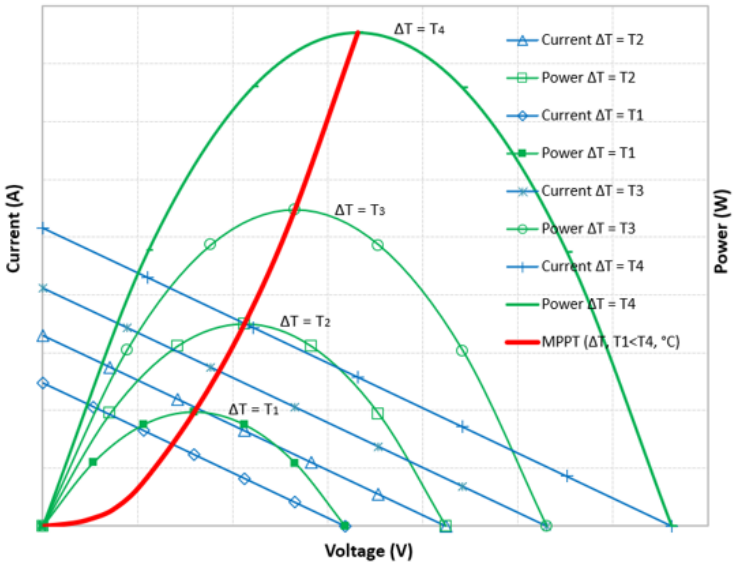

Figure 3. The I-V, P-V, and MPPT curves.

Since the modules used in TEG systems have low efficiency, it is necessary to obtain maximum power from TEG waste heat recovery systems by using power regulating methods. The power from the TEGs is transferred through the load resistor, so in (3) the power is written in terms of internal resistance and load resistance. The load resistance and internal resistance must be equal ($R_L = R_{int}$) with reference to the maximum power theorem for the most efficient power transfer [25].

The energy obtained from TEGs is directly dependent on the temperature difference, and TEGs are generally used in regions where the temperature differences are not linear. The temperature change not only changes the power produced by the TEGs but also changes the internal resistance [11] and Seebeck coefficients [16] of the TEGs.

As can be understood from (1), the voltage produced by the TEG changes with the Seebeck coefficient which changes depending on the temperature. If the Seebeck coefficient remained constant, it would be possible to obtain the same energy whenever the temperature difference is the same. However, the impossibility of this situation proves that the Seebeck coefficient changes depending on the temperature. In (3), in cases where R_{int} of the TEG changes, it is necessary to change R_L connected to the TEG to be equal to the load for obtaining maximum generation from TEG systems. In this case, as R_L of the TEG cannot be changed continuously, it is hard to obtain the maximum generation from the TEG systems. Therefore, some exclusive electronic components are required to equalize R_{int} of the TEG with R_L [26]. Therefore, a DC-DC converter embedded MPPT software is used between the TEG and the load, which is utilized to generate maximum power and constant voltage from the TEG and also performs impedance matching [27].

In this study, manufacturer data of TGM-199-1.4-0.8 module is used as TEG module. The TEG system, designed by connecting five modules in series, is modeled in Simulink® according to these module features. The specifications of the TEG module and the specifications of the TEG system are given in Table 1.

Table 1. Specifications of TEG module and TEG system.

Characteristics	**TGM-199-1.4-0.8**	**TEG system**
TE couples (N)	199	199
Thermoelectric modules	1	Five in series
Output Power at MPP (P_{MPP})	11.4 W	57 W
Output Voltage at MPP (V_{MPP})	4.1 V	20.5 V
Output Current at MPP (I_{MPP})	2.8 A	2.8 A
Open circuit voltage (V_{OC})	8.19 V	41 V
Short circuit current (I_{SC})	5.61 A	5.61 A
Internal Resistance	1.46 Ω	7.3 Ω
Hot-side temperature (T_H)	200 °C	200 °C
Cold-side temperature (T_C)	30 °C	30 °C

3. Maximum power point tracking

MPPT is a well-known control method that enables power systems to operate at their maximum power capacity under various conditions. The use of MPPT control algorithms in TEG systems is very important due to the low efficiency of TEGs. According to the maximum power transfer theorem [28], a maximum power is taken from the TEG at a certain value of the load connected to the TEG terminals. This defined value changes with the value of the TEG's internal resistance. MPPT control algorithms are used with DC-DC converters to match the impedance between the TEG and the load, so the TEG will always run at the MPP. According to the MPPT algorithm used in MPPT methods, some variables are constantly tracked. The power delivered through the load resistor varies depending on the load resistor value. In order to apply MPPT methods with a converter, it should be taken into account that the I-V and P-V curves of the TEG system deal with the load resistance. Maximum power from TEG is provided at MPP. MPP displaces with changes in load resistance

and changes with a temperature gradient between surfaces of TEG system. The increase in the temperature difference between the waste heats of the TEG system increases the MPP value of the electrical energy to be obtained from the system. As this temperature difference increases, the efficiency value of the TEG system increases and is explained by a second order function [29]. Therefore, the nonlinear situation in TEG yield should be considered in MPP software.

The most important criterion for the application of MPPT algorithms is the equalization of the TEG internal resistance and the load resistance values connected to the TEG. This situation is called load matching. TEG reaches MPP when $(R_L = R_{int})$ condition is met. In other words, maximum power transfer is provided from the TEG to the load. In this study, Perturb and Observe (P&O) MPPT algorithm [30], which is frequently used in the literature, was preferred as the MPPT algorithm and the flowchart of the method is given in Figure 4. In the P&O MPPT method, there is a continuous change of the duty cycle (D) value to capture the MPP point. The greater the range of changes in the D value, the greater the fluctuation around the MPP. On the other hand, when the ranges of change in D value are small, it takes a little more time to catch the MPP value. However, the fluctuations in the MPP value decrease. In the application of this method, current and voltage values should be detected with a sensor in order to determine the TEG output power. In addition, in the application of this method, it is necessary to constantly compare the new power value $(P(k))$ measured with the previous power value $(P(k-1))$ [31].

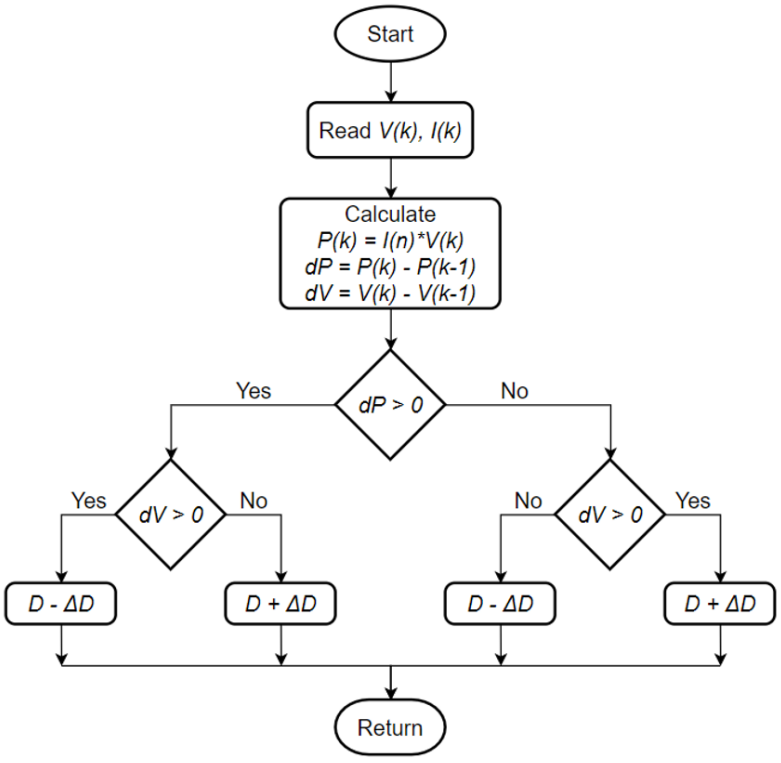

Figure 4. Perturb & observe algorithm [32].

4. Boost converter design

The boost converter given in Figure 5 is one of the nonisolated converters. They are used to increase the input voltage. Of course, as this voltage value increases, the current value decreases. It is placed between the TEG systems and the load to use MPPT algorithms. Thus, they provide the impedance matching between the TEG system and the load. This impedance matching is accomplished by changing the D value of the switch in the converter. Thus, together with the load resistor, they act like a programmable resistor equal to the internal resistance of the TEG [9].

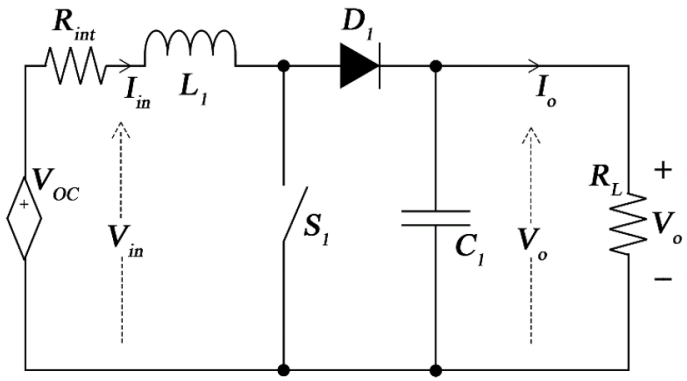

Figure 5. DC-DC boost converter.

Boost converters change the input voltage to the output voltage with a certain ratio value. This ratio is given in the equations below. The D value is very decisive here.

$$\frac{V_o}{V_{in}} = \frac{I_{in}}{I_o} = \frac{1}{1-D}, \tag{5}$$

$$V_{in} = V_o(1-D), \tag{6}$$

$$I_{in} = \frac{I_o}{1-D}. \tag{7}$$

The meanings of the values used in the above equations are as follows: V_{in} is the input voltage of the converter, V_o is the output voltage of the converter, I_{in} is the input current of the converter, and I_o is the output current of the converter. Using these equations, changing the value of D indicates that the load of the TEG can be made programmable. This equation is given below [9]:

$$R_{PROG} = \frac{V_{\text{in}}}{I_{\text{in}}} = \frac{V_o(1-D)}{I_o/(1-D)} = \frac{V_o(1-D)^2}{I_o} = R_L(1-D)^2. \tag{8}$$

(8) shows that the converter behaves like a programmable resistor and this resistor can be changed depending on the load resistance by adjusting the duty cycle. As can be understood from this formula, for R_{PROG} resulting from impedance matching to be equal to TEG's internal resistance, the load resistance must be greater than the TEG's internal resistance. Otherwise, impedance matching cannot be performed [33].

Manufacturer data of TGM-199-1.4-0.8 TEG module is used for boost converter design. Table 2 shows the maximum design parameters, and the inductor and capacitor values of the converter designed according to these parameters.

Table 2. Boost convertor design parameters.

Parameter	Value	Description
P_{MPP}	57 W	Maximum power
P_{conv}	60 W	Power of converter (P_{max})
V_{in}	20.5 V	Input voltage
R_L	10 Ω	Load resistance
V_o	24.5 V	Maximum output voltage
I_o	2.45 A	Maximum output current
ΔI_L	30% of I_o	Maximum ripple current
ΔV_o	2% of V_o	Maximum voltage ripple at MPP
η	0.9	Efficiency
f_s	20 kHz	Switching frequency
L_1	220 μH	Inductor
C_1	2200 μF	Capacitor

5. Simulink® model of thermoelectric generator module

The proposed Simulink® model uses the manufacturer data of the TEG module and produces results compatible with these data. Firstly, the information presented graphically in the manufacturer's data is converted into usable data in MATLAB® with curve fitting methods and methods of obtaining data from the graph. These data are then used as comparison tables in Simulink®. Figure 6 shows the Simulink® model and the internal structure of the TEG module. Figure 6a is a subsystem representing the modeled thermoelectric module. On the left side of this subsystem, there are two inputs for specifying the hot surface and cold surface temperatures, and there is an input to specify the number of modules to use. If this input is given a value of one, the subsystem can be used as a single module. When the input value is two or more, the subsystem indicates that as many serially connected modules as this value are used in the TEG system. Thus, the number of modules can be increased to obtain the desired power. The (+) and (-) terminals on the right side of the subsystem represent the output connections of the thermoelectric module. Converters can be easily connected to these terminals and used with the designed model. In addition, measurements such as open circuit voltage and short circuit current of the module are made through these terminals. If it is desired to connect the modules in parallel in the TEG system to be installed, two separate subsystems can be connected to each other by matching the (+) and (-) terminals of the modules.

From the output voltage formula of a TE given in (1), the Seebeck coefficients of the pn pairs in the TEG module are calculated as shown in (9).

$$\alpha_{pn} = \frac{V_{\text{out}}}{N\Delta T}, \tag{9}$$

where α_{pn} is the Seebeck coefficient of a pn pair. The Seebeck coefficient of a TEG module is $N\alpha_{pn}$. The number of pn pairs in the TEG module is expressed with N and there are 199 pn pairs in the TEG module used in this study. V_{out} represents the voltage produced by the module at the temperature difference of $\Delta T = T_H - T_C$ and is obtained by importing the manufacturer's data into the computer environment.

Figure 6b shows the internal structure of the subsystem. An output voltage is generated according to (1) using surface temperatures, module number, and Seebeck coefficient data. A dependent source, highlighted in orange, represents that the voltage produced is temperature-dependent. The important point in this model is that the Seebeck coefficient is temperature sensitive. Using the manufacturer's data of the modeled module, Seebeck coefficients at all temperature values are calculated according to (9) and placed in the Look-up table at the bottom of Figure 6b. Thus, the most accurate Seebeck coefficient can be used at any cold surface and any hot surface temperature.

Another important point in this model is that it does not ignore the temperature-dependent variation of the internal resistance of the module. The variable resistor in the upper right of Figure 6b represents the internal resistance of the modeled module. According to (3), the power obtained from the TEG module directly depends on the internal resistance. It is extremely important to use an internal resistance model that changes depending on cold and hot surface temperatures in order to get accurate results. Therefore, the Look-up table prepared using the R_{int} values found in the manufacturer's data, as in the Seebeck coefficient, is placed at the top of Figure 6b. By using the temperature information, the R_{int} values closest to reality are used in the model through comparison tables. Figure 7 shows the manufacturer's data and the R_{int} values generated by the curve fitting method. The R_{int} data obtained by the curve fitting method are integrated into the Look-up tables in the subsystem in Figure 6b and the correct value of R_{int} is used in the model according to the changing surface temperatures. Figure 7 shows the manufacturer data of the TEG's internal resistance with respect to hot side and cold side temperatures and the estimated curves passing through the points closest to these data. The curves are optimized from the fifth order for the best results. After the optimization, the data on the R_{int} curves generated with the equation coefficients estimated are integrated into the Look-up tables in the subsystem for the internal resistances in Figure 6b. Thus, the datasheet values of R_{int} at certain temperatures can be used as almost the same value in simulations.

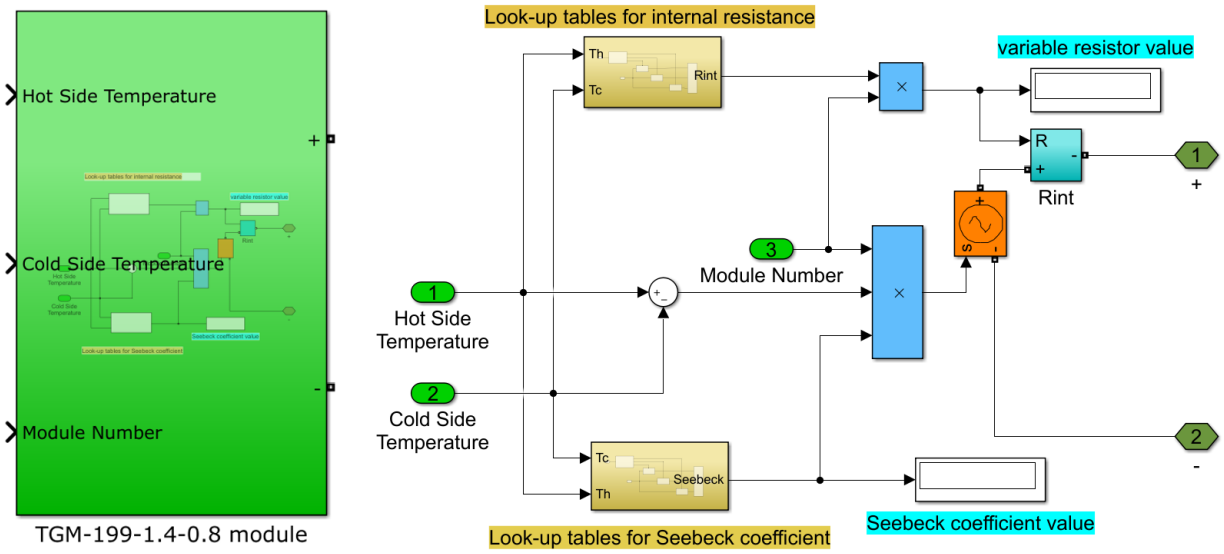

Figure 6. (a) Simulink® model of the TEG module (b) Internal structure of the TEG module.

This study uses data presented in the manufacturer's data for cold surface temperatures of 30 °C, 50 °C, and 80 °C. The hot surface temperature is increased up to 220 °C starting from 20 °C above the cold surface temperature. The Seebeck coefficients of each pn pair of the module, whose cold surface temperature is kept

constant at 30 °C, 50 °C, and 80 °C, appear as in the graph given in Figure 8 as a result of the calculations. The data in this graph is made into regular data by the curve fitting method. This data is multiplied by the number of pn pairs to calculate the Seebeck coefficient of a module and embedded in the Look-Up tables in the subsystem shown in Figure 6b. Thus, the Seebeck coefficient used in the simulation environment changes as the temperature changes and more realistic results can be obtained.

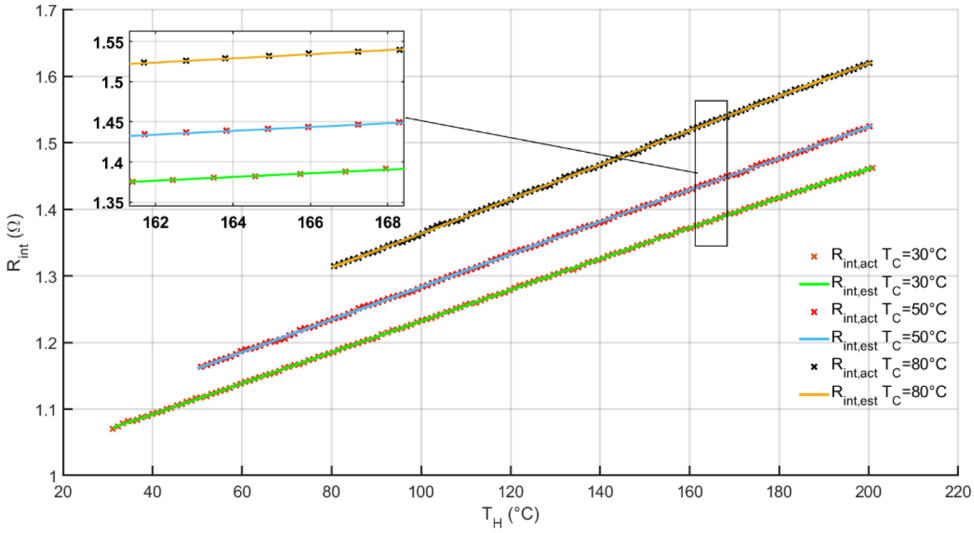

Figure 7. Manufacturer R_{int} data compared to the R_{int} values generated by the curve fitting method.

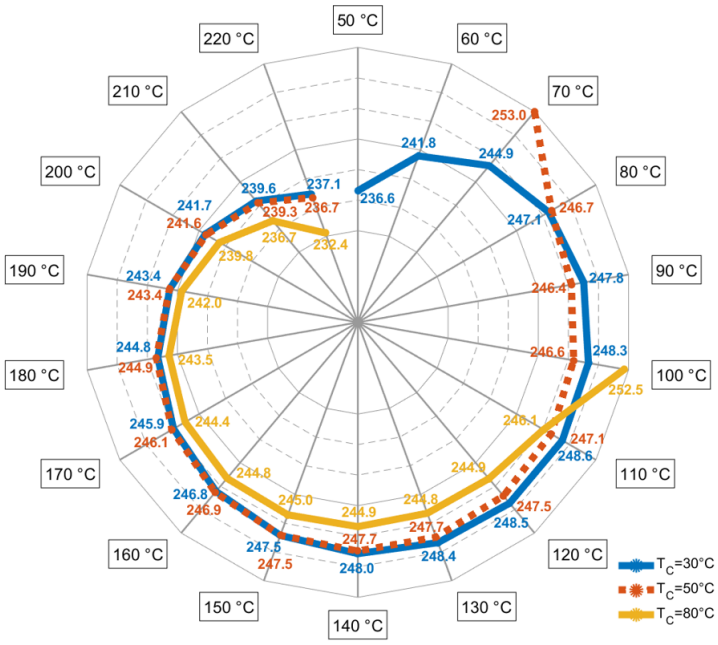

Figure 8. The Seebeck coefficients ($\mu V/K$) calculated at certain hot surface temperatures for a pn pair.

6. Simulation results and discussions

In this section, the tests and simulation results of the fully modeled TEG module with the Simulink® model are presented and discussed. First of all, when the Seebeck coefficients under different temperature conditions presented in the image in Figure 8 are examined, it is observed that almost all of them are different from each other. The Seebeck coefficient, which is one of the most important parameters to be considered while modeling TEG modules in Simulink®, can cause large deviations in TEG systems where a large number of modules are connected in series/parallel. Table 3 presents the minimum, maximum, and average values of the Seebeck coefficient according to the cold surface temperature. The average values of the Seebeck coefficient are close to each other. It is observed that at $T_C = 30°C$ when T_H is increased from 50 °C to 220 °C, the Seebeck coefficient increases up to 110 °C and takes its maximum value, then its value decreases again. At $T_C = 50°C$, when T_H is increased from 70 °C to 220 °C, if the instability at 70 °C is ignored, it can be said that the Seebeck coefficient increases up to 140 °C and takes its maximum value, then decreases again. However, at $T_C = 80°C$, the Seebeck coefficient decreases continuously as T_H is increased from 100 °C to 220 °C. In addition, as the cold surface temperature increases, the difference between the maximum value of the Seebeck coefficient relative to the hot surface temperature and the minimum value increases.

On the other hand, considering the Seebeck coefficient, in many studies a connection is made between the concept of the temperature difference and the power obtained from TEG. However, as seen in Table 4, even if the temperature difference is constant, the Seebeck coefficient is different due to the difference in surface temperatures. In Table 4, the Seebeck coefficient is not the same in any of the same constant temperature difference conditions. The Seebeck coefficients given in the tables are for a pn pair. Since there are 199 pn pairs in the TEG module considered in this study, the Seebeck coefficient of the TEG module can be calculated by multiplying the given coefficients by 199. Although the given Seebeck coefficients seem to be close to each other, deviations occur in the results due to the aforementioned calculation. Considering that more than one module is used in a TEG system, the inaccuracies in the results will increase as the number of modules.

Table 3. Seebeck coefficient values with respect to cold surface temperature.

T_C	$\alpha_{pn}(\mu V/K)$			
	Min	Max	Difference	Average
30 °C	236.6	248.6	12	242.6
50 °C	236.7	253	16.3	244.85
80 °C	232.4	252.5	20.1	242,45

Table 4. Seebeck coefficient values with respect to temperature difference.

T_C	T_H	ΔT	$\alpha_{pn}(\mu V/K)$
30 °C	80 °C	50 °C	247.1
50 °C	100 °C		246.6
80 °C	130 °C		244.8
30 °C	110 °C	80 °C	248.6
50 °C	130 °C		247.7
80 °C	160 °C		244.8
30 °C	130 °C	100 °C	248.4
50 °C	150 °C		247.5
80 °C	180 °C		243.5
30 °C	170 °C	140 °C	245.9
50 °C	190 °C		243.4
80 °C	220 °C		232.4

Figure 9 shows the open-circuit voltage and short-circuit current measurements of the Simulink® model of the TEG module. These measurements are taken under $T_C = 30°C$ and $T_H = 200°C$ conditions, as there are numerical results in the manufacturer's data. At the moment of impedance matching, it is stated in the

manufacturer's data that under these conditions the load current is 2.8 A, the load voltage is 4.1 V, and the output power is 11.4 W. The TEG module reaches these values in MPP. It is known that in MPP the load current is half the short-circuit current and the load voltage is half the open-circuit voltage [9]. Accordingly, the short-circuit current of the TEG module is 5.6 A and the open-circuit voltage is 8.2 V. According to the test results presented in Figure 9, the short-circuit current and open-circuit voltage are measured as $I_{SC} = 5.593A$ and $V_{OC} = 8.179V$, respectively. The error rate between manufacturer data and simulation results is 0.125% and 0.256% for I_{SC} and V_{OC}, respectively.

The I-V and P-V characteristics of the designed TEG module model are shown in Figure 10. In the simulation at this step, the cold surface temperature is 30 °C and the hot surface temperature is 200 °C, as in the manufacturer's data. The point where the current graph cuts the x-axis gives the value of the open-circuit voltage, and the point where it cuts the y-axis gives the value of the short circuit current. Moreover, at the MPP point, the voltage is half the open-circuit voltage and the current is half the short-circuit current. The characteristic curves of the model agree with the manufacturer's numeric data in Table 1 and meet the test results shown in Figure 9.

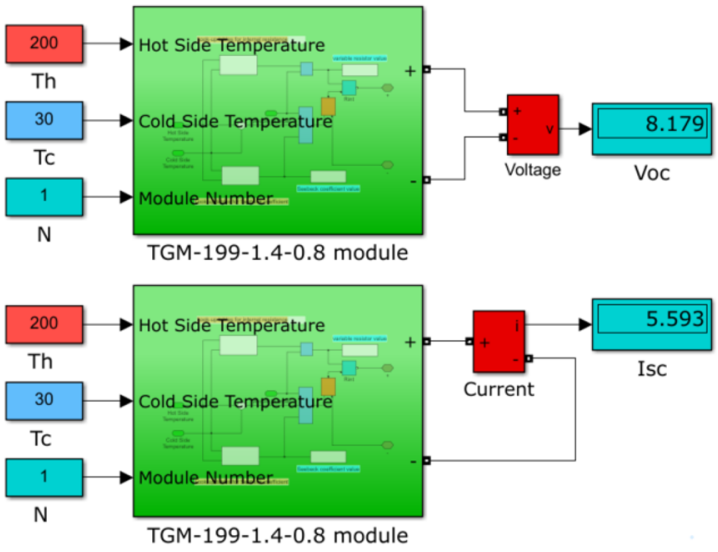

Figure 9. Open circuit voltage and short circuit current of the modeled TEG module.

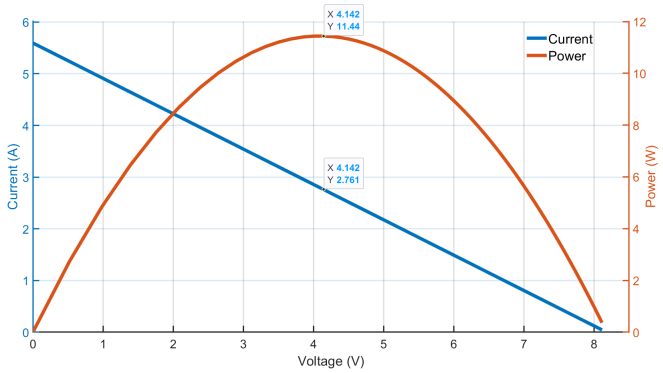

Figure 10. The I-V and P-V curves of the modeled TEG module.

The modeled module is tested at different combinations of hot and cold surface temperatures. Figure 11 shows the comparison of the results obtained from the simulation with the manufacturer's data of the module when the T_C is kept constant at 30 °C, 50 °C, 80 °C, respectively, and the T_H is increased up to 200 °C. It can be clearly seen that the simulation result gives almost the same result as the manufacturer's actual data. In addition, the error values between the simulation results and the manufacturer's data for each cold surface temperature are given in graphs on the right of the figure. The data in these graphs are used to calculate the MAPE values of the Simulink® model. MAPE is a metric used to determine the accuracy of a forecasting system. Actual data and estimated values are used to calculate MAPE. In order to verify the accuracy of the module modeled in this study, TEG Simulink/MATLAB® model data are compared with commercially available TEG data at different temperatures and MAPE values are calculated. For cold surface temperatures of 30 °C, 50 °C, and 80 °C, the MAPEs are 0.5104%, 0.7837%, and 2.0952%, respectively. Even the largest MAPE value of the Simulink® model designed in this study is considerably lower than the acceptable 5% value. Especially in simulations where the cold surface temperature is 30 °C and the hot surface temperature is higher than 180 °C, the error is very small. Therefore, these error graphs and the MAPE values quite validate the Simulink® model.

By using the TEG system, which consists of five TEG modules connected in series, the characteristics of which are given in Table 1, the effects of TEG's internal resistance and Seebeck coefficient on the system are investigated. In order to provide the maximum power from the TEG, a boost converter is used, which is installed with the components calculated using the design criteria given in Table 2 mentioned in the fourth section. By connecting a fixed 15Ω load to the boost converter terminals, power is obtained from the TEG over the load. The duty cycle of the switching element of the boost converter is adjusted with the P&O MPPT algorithm in order to obtain the maximum power from the system. The TEG system put together in Simulink® using the designed model, the designed boost converter, the MPPT algorithm, and the load is shown in Figure 12.

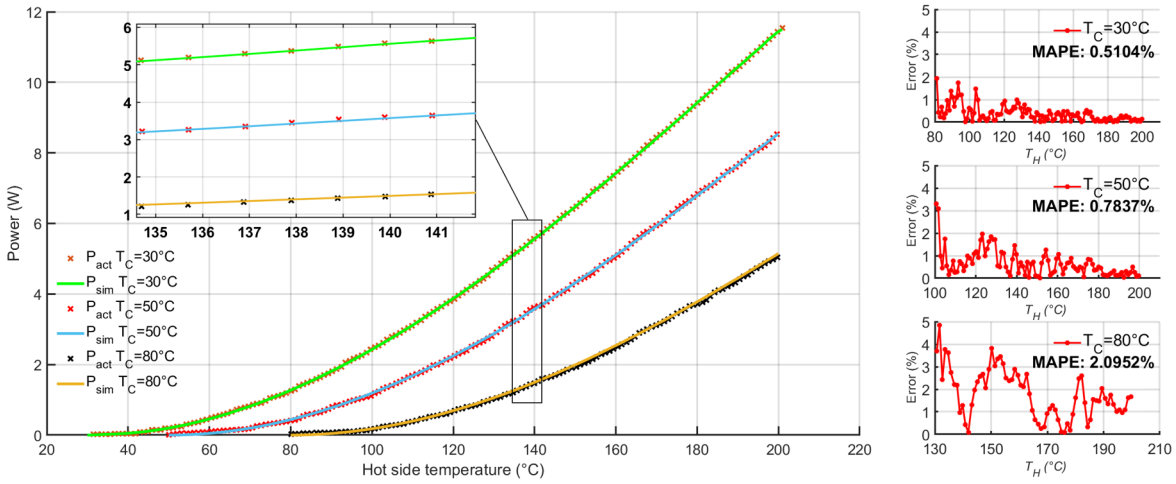

Figure 11. Comparison of the datasheet power data of the module and the power data produced by the simulation result of the module modeled in Simulink®, and error graphs with MAPE values.

In Figure 13, the powers obtained from the system are compared by using the fixed R_{int} value and the R_{int} value modeled depending on the temperature when T_H is constant at 200 °C and T_C is 30 °C, 50 °C, 80 °C. The fixed R_{int} value is the value given for $T_C = 30°C$ and $T_H = 200°C$ in the manufacturer's data and is 1.46Ω. Therefore, the simulation results for $T_C = 30°C$ are the same in both R_{int} conditions. However, when

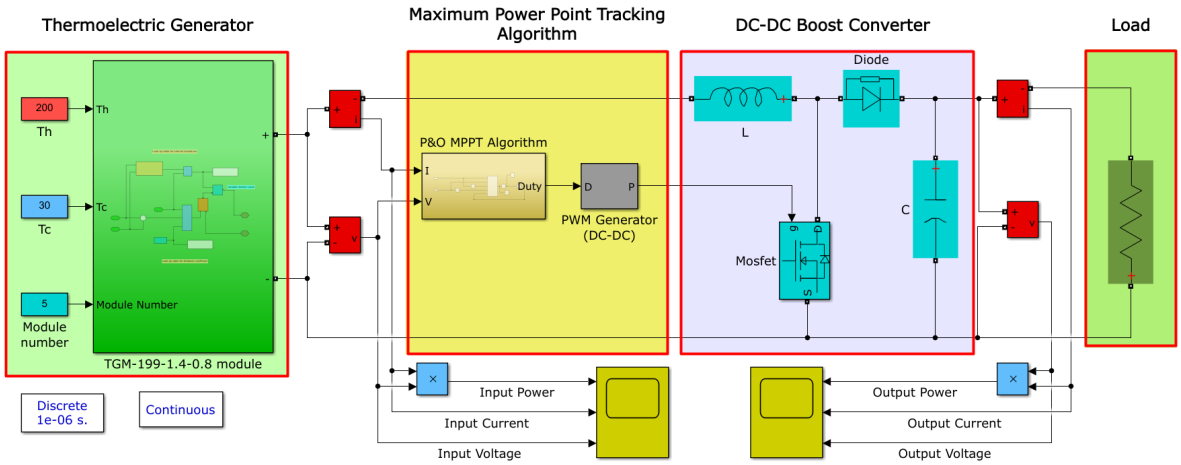

Figure 12. The TEG system modeled in Simulink®.

the T_C value is 50 °C or 80 °C, the results obtained with a fixed R_{int} value are quite different from the actual results, as the R_{int} value will change due to temperature. In the simulation with five serial modules, the power obtained from the TEG system is expected to be five times the power obtained from a module. In other words, five times the power values shown in Figure 11 can be obtained. When Figure 13 is examined, it is observed that the powers obtained with the temperature-dependent R_{int} values are five times closer to the power curves given in Figure 11. In addition, the power obtained with the R_{int} values changing depending on the temperature is quite close to the power that can be obtained from the system in reality. It can be understood from this that the internal resistance of the TEG should be modeled depending on the temperature. Even if the amount of error for a module is seen to be negligible, the error margin increases much more with the losses in systems designed using much more TEG modules.

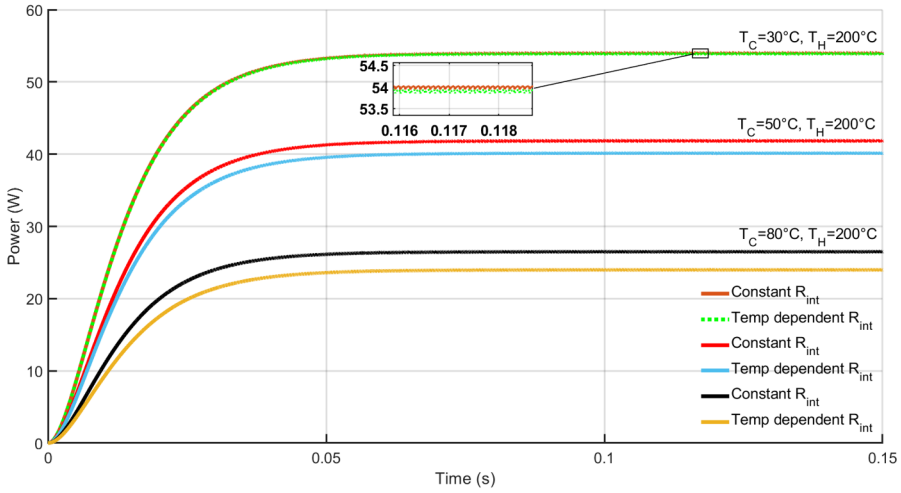

Figure 13. Comparison of constant internal resistance and temperature-sensitive internal resistance in TEG system.

Similarly, a simulation is performed to see the effect of the constant Seebeck coefficient and the temperature-sensitive Seebeck coefficient on the system. In Figure 14, the powers obtained from the system are compared by using the fixed Seebeck coefficient and the Seebeck coefficient modeled depending on the temperature when

T_H is constant at 200 °C and T_C is 30 °C, 50 °C, 80 °C. An average value is used as the constant Seebeck coefficient. As seen in Figure 8, the Seebeck coefficient for $T_C = 30°C$ first increases and then decreases as the hot surface temperature increases. Therefore, the constant Seebeck coefficient will be higher for $T_H = 200°C$ and the power obtained from the system will be higher than the actual one. When the design criteria and the capacity of the TEG system are examined, the maximum power that can be obtained from the TEG is 57 W under $T_C = 30°C$ and $T_H = 200°C$ conditions. However, it is seen in Figure 14 that 58.5 W is obtained from the system due to the constant Seebeck coefficient. In other words, 2.63% more power is obtained from the TEG system as a result of the simulation, due to the use of the wrong Seebeck coefficient. Since this will not be possible in reality, it is very important to use the most appropriate value of the Seebeck coefficient in simulations. Similar deviations are also valid for $T_C = 50°C$ and 80 °C. Moreover, another result observed in Figure 14 is that the error increases as the temperature difference increases. It is one of the most important elements to be considered in the Simulink® model, as the effect of the Seebeck coefficient increases exponentially when the temperature difference increases and especially in TEG systems where too many modules are used.

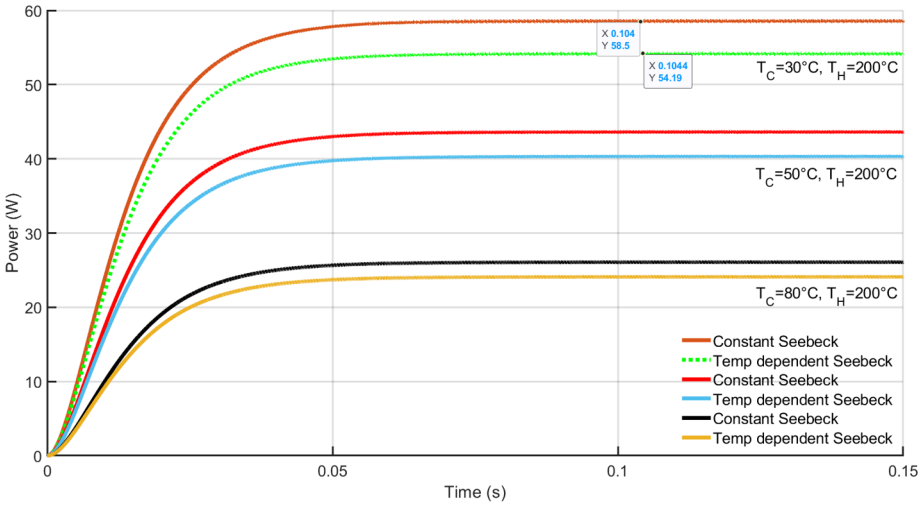

Figure 14. Comparison of constant Seebeck coefficient and temperature-sensitive Seebeck coefficient in TEG system.

7. Conclusion

Developed using the Seebeck phenomenon, TEGs convert waste heat into energy, and their performance changes according to surface temperatures. The Seebeck coefficient is a parameter that changes depending on the temperature. However, in many studies, the Seebeck coefficient is either not mentioned or simulations are made using a fixed Seebeck coefficient. Using the Seebeck coefficient as a constant means that the same power can be obtained at every same temperature difference. However, TEGs have different internal resistance values and Seebeck coefficients according to their surface temperatures. Therefore, different powers are obtained from TEGs in many same temperature difference combinations. Due to the nature of TE materials in the structure of TEGs, their internal resistances and Seebeck coefficients that change with temperature have to be adapted to the simulation environment in order to obtain realistic and accurate results. In this study, a TEG module is modeled with reference to manufacturer data. The simulations are run at three different cold surface temperatures, 30 °C, 50 °C, and 80 °C. The hot surface temperature varies according to the simulation. That is, to obtain the results in Figures 7 and 11, simulations are run for all values of hot surface temperatures between 30 °C

and 200 °C. On the other hand, to obtain the results in Figure 8, the hot surface temperatures are increased in 10 °C steps from 50 °C to 200 °C. Unlike these simulations, the comparison results in Figures 9, 13, and, 14 are obtained when the hot surface temperature is constant at 200 °C. Firstly, the internal resistance of the TEG module is modeled for each hot surface and cold surface temperature combination. The internal resistance, which is modeled with the curve fitting method using real data, produces almost identical results to the manufacturer's data. Then, the Seebeck coefficient, which is not found in the manufacturer's data, is calculated for each temperature value using other information from the manufacturer's data. As a result of the tests made with the modeled module, the open-circuit voltage and short circuit current of the TEG module gives a result in accordance with the manufacturer's data with negligible error. I-V and P-V graphs obtained by simulation using variable load capture the open-circuit voltage, short circuit current, and maximum power point at the right points. The result of these simulations is very similar to the matched load resistor output power data in the manufacturer data. The MAPE values calculated to verify the conformity of the modeled module with the actual values are 0.5104%, 0.7837%, and 2.0952% for cold surface temperatures of 30 °C, 50 °C, and 80 °C, respectively. Even the highest MAPE value is well below the 5% fitness value accepted in the literature. In addition, it is explained with simulations that the results are largely inaccurate when constant internal resistance and constant Seebeck coefficients are used. However, as indicated in the tables, even if the same temperature difference value is achieved by changing the surface temperatures, the value of the Seebeck coefficient changes. Because the value of the Seebeck coefficient depends on the surface temperatures, not the temperature difference. In conclusion, this study, which deals with a modeled and verified TEG module, touches on important points in terms of getting more accurate and realistic results for researchers working with TEG systems in the simulation environment. The designed TEG module model is also open to mechanical development such as heat flow modeling and thermal conductivity modeling with multidisciplinary studies.

Acknowledgment

This work was supported by Research Project Coordination Unit of The Manisa Celal Bayar University (Project Number: 2022-012).

References

[1] Mamur H, AHISKA R. A review: Thermoelectric generators in renewable energy. International Journal of Renewable Energy Research (IJRER). 2014;4 (1):128-136

[2] Siddique ARM, Mahmud S, Heyst BV. A review of the state of the science on wearable thermoelectric power generators (TEGs) and their existing challenges. Renewable and Sustainable Energy Reviews. 2017;73:730-744. doi:10.1016/j.rser.2017.01.177

[3] Champier D. Thermoelectric generators: A review of applications. Energy Conversion and Management. 2017;140:167-181. doi:10.1016/j.enconman.2017.02.070

[4] He W, Zhang G, Zhang X, Ji J, Li G et al. Recent development and application of thermoelectric generator and cooler. Applied Energy. 2015;143:1-25

[5] Twaha S, Zhu J, Maraaba L, Huang K, Li B et al. Maximum Power Point Tracking Control of a Thermoelectric Generation System Using the Extremum Seeking Control Method. Energies. 2017;10 (12):2016. doi:10.3390/en10122016

[6] Yeler O, Koseoglu MF. Energy efficiency and transient-steady state performance comparison of a resistance infant incubator and an improved thermoelectric infant incubator. Engineering Science and Technology, an International Journal. 2022;31:101055. doi:10.1016/j.jestch.2021.09.001

[7] Ahiska R, Ahiska K. New method for investigation of parameters of real thermoelectric modules. Energy Conversion and Management. 2010;51 (2):338-345. doi:10.1016/j.enconman.2009.09.030

[8] Bhuiyan MRA, Mamur H, Üstüner MA, Dilmaç ÖF. Current and Future Trend Opportunities of Thermoelectric Generator Applications in Waste Heat Recovery. Gazi University Journal of Science. 2022;35 (3):896-915. doi:10.35378/gujs.934901

[9] Mamur H, Üstüner MA, Bhuiyan MRA. Future perspective and current situation of maximum power point tracking methods in thermoelectric generators. Sustainable Energy Technologies and Assessments. 2022;50:101824. doi:10.1016/j.seta.2021.101824

[10] Chen WH, Lin YX. Performance comparison of thermoelectric generators using different materials. Energy Procedia. 2019;158:1388-1393. doi:10.1016/j.egypro.2019.01.339

[11] Montecucco A, Knox AR. Maximum Power Point Tracking Converter Based on the Open-Circuit Voltage Method for Thermoelectric Generators. IEEE Transactions on Power Electronics. 2015;30 (2):828-839. doi:10.1109/TPEL.2014.2313294

[12] Kwan TH, Wu X. Maximum power point tracking using a variable antecedent fuzzy logic controller. Solar Energy. 2016;137:189-200. doi:10.1016/j.solener.2016.08.008

[13] Houssein EH, Helmy BE din, Rezk H, Nassef AM. An efficient orthogonal opposition-based learning slime mould algorithm for maximum power point tracking. Neural Comput & Applic. 2022;34 (5):3671-3695. doi:10.1007/s00521-021-06634-y

[14] Tsai HL, Lin JM. Model Building and Simulation of Thermoelectric Module Using Matlab/Simulink. Journal of Elec Materi. 2010;39 (9):2105-2111. doi:10.1007/s11664-009-0994-x

[15] Kennedy C. Simulink Model of TEG module. Accessed April 14, 2022. https://www.mathworks.com/matlabcentral/fileexchange/74694-simulink-model-of-teg-module

[16] Burnete NV, Mariasiu F, Moldovanu D, Depcik C. Simulink Model of a Thermoelectric Generator for Vehicle Waste Heat Recovery. Applied Sciences. 2021;11 (3):1340. doi:10.3390/app11031340

[17] Hsu CT, Huang GY, Chu HS, Yu B, Yao DJ. An effective Seebeck coefficient obtained by experimental results of a thermoelectric generator module. Applied Energy. 2011;88 (12):5173-5179. doi:10.1016/j.apenergy.2011.07.033

[18] Photoon R aroon, Wichakool W. System Modelling and Controller designed for Thermoelectric Generator using a First Order Plus Dead Time. ECTI Transactions on Computer and Information Technology (ECTI-CIT). 2016;10 (1):80-87. doi:10.37936/ecti-cit.2016101.56399

[19] Faria MAA, Stecanella PAJ, Domingues EG, Gomes PHG, Calixto WP et al. Modeling, simulation and control of a thermoelectric generator. In: 2015 IEEE 15th International Conference on Environment and Electrical Engineering (EEEIC). ; 2015:1373-1378. doi:10.1109/EEEIC.2015.7165370

[20] El-Shahat A, Bhuiyan MdSR. Thermoelectric Generator Performances and Efficiency Analysis Integrated with MPPT Techniques. In: 2021 International Conference on Sustainable Energy and Future Electric Transportation (SEFET). 2021:1-7. doi:10.1109/SeFet48154.2021.9375713

[21] Wang N, Zhang J, Ni H, Jia H, Ding C. Improved MPPT System based on FTSMC for Thermoelectric Generator Array under Dynamic Temperature and Impedance. IEEE Transactions on Industrial Electronics. Published online 2022:1-1. doi:10.1109/TIE.2022.3152007

[22] Markowski PM. Multilayer thick-film thermoelectric microgenerator based on LTCC technology. Microelectronics International. 2016;33 (3):155-161. doi:10.1108/MI-05-2016-0038

[23] Jaziri N, Boughamoura A, Müller J, Mezghani B, Tounsi F et al. A comprehensive review of Thermoelectric Generators: Technologies and common applications. Energy Reports. 2020;6:264-287. doi:10.1016/j.egyr.2019.12.011

[24] Wu H, Sun K, Zhang J, Xing Y. A TEG Efficiency Booster with Buck–Boost Conversion. Journal of Elec Materi. 2013;42 (7):1737-1744. doi:10.1007/s11664-012-2407-9

[25] Remeli MF, Tan L, Date A, Singh B, Akbarzadeh A. Simultaneous power generation and heat recovery using a heat pipe assisted thermoelectric generator system. Energy Conversion and Management. 2015;91:110-119. doi:10.1016/j.enconman.2014.12.001

[26] Mamur H, Ahiska R. Application of a DC–DC boost converter with maximum power point tracking for low power thermoelectric generators. Energy Conversion and Management. 2015;97:265-272. doi:10.1016/j.enconman.2015.03.068

[27] Yamada H, Kimura K, Hanamoto T, Ishiyama T, Sakaguchi T et al. A Novel MPPT Control Method of Thermoelectric Power Generation with Single Sensor. Applied Sciences. 2013;3 (2):545-558. doi:10.3390/app3020545

[28] Semmlow J. Chapter 11 - Circuit Reduction: Simplifications. In: Semmlow J, ed. Signals and Systems for Bioengineers (Second Edition). Biomedical Engineering. Academic Press; 2012:471-517. doi:10.1016/B978-0-12-384982-3.00011-0

[29] Bjørk R, Nielsen KK. The performance of a combined solar photovoltaic (PV) and thermoelectric generator (TEG) system. Solar Energy. 2015;120:187-194. doi:10.1016/j.solener.2015.07.035

[30] Rajamand S. A novel sliding mode control and modified PSO-modified P&O algorithms for peak power control of PV. ISA Transactions. Published online April 11, 2022. doi:10.1016/j.isatra.2022.04.009

[31] Kamran M, Mudassar M, Fazal MR, Asghar MU, Bilal M et al. Implementation of improved Perturb & Observe MPPT technique with confined search space for standalone photovoltaic system. Journal of King Saud University - Engineering Sciences. 2020;32 (7):432-441. doi:10.1016/j.jksues.2018.04.006

[32] Mamur H, Çoban Y. Detailed modeling of a thermoelectric generator for maximum power point tracking. Turkish Journal of Electrical Engineering and Computer Sciences. 2020;28 (1):124-139. doi:10.3906/elk-1907-166

[33] Dileep G, Singh SN. Selection of non-isolated DC-DC converters for solar photovoltaic system. Renewable and Sustainable Energy Reviews. 2017;76:1230-1247. doi:10.1016/j.rser.2017.03.130